Building Simulation

Seventh International IBPSA Conference
Rio de Janeiro, Brazil
August 13-15, 2001

FURTHER DEVELOPMENTS IN THE CONFLATION OF CFD AND BUILDING SIMULATION

Beausoleil-Morrison I[(1)], Clarke J A[(2)], Denev J[(3)]
Macdonald I A[(2)], Melikov A[(4)], Stankov P[(3)]

(1) CETC, Natural Resources Canada, ibeausol@nrcan.nrcan.gc.ca
(2) ESRU, University of Strathclyde, Scotland, esru@strath.ac.uk
(3) Technical University of Sofia, Bulgaria, denev@cfdc-hp2.vmei.acad.bg
(4) Centre for Indoor Environment and Energy, Technical University of Denmark, melikov@et.dtu.dk

ABSTRACT

To provide practitioners with the means to tackle problems related to poor indoor environments, building simulation and computational fluid dynamics can usefully be integrated within a single computational framework.

This paper describes the outcomes from a research project sponsored by the European Commission, which furthered the CFD modelling aspects of the ESP-r system. The paper summarises the form of the CFD model and describes the method used to integrate the thermal and flow domains.

Keywords: Building performance simulation, computational fluid dynamics, integrated modelling.

INTRODUCTION

Within building energy simulation two modelling approaches are extant: nodal networks and computational fluid dynamics.

Within the former method, as implemented within the ESP-r system (Clarke and Hensen 1991), the building and its air handling plant are treated as a collection of nodes representing rooms (or parts of rooms), equipment connection points, ambient conditions etc. Inter-nodal connections are then defined to represent components such as cracks, doors, windows, fans, ducts, pumps etc. Each component is assigned a model that gives the mass flow rate as a function of pressure difference. Consideration of the conservation of mass at each node leads to a set of non-linear equations that can be integrated over time to characterise the flow domain.

Although well adapted for building energy application, the nodal network method is limited when it comes to consideration of indoor comfort and air quality: because momentum effects are neglected, intra-room air movement cannot be studied; and, as a result of the low resolution, local surface convection heat transfer is poorly represented. To overcome these limitations, it is necessary to introduce a CFD model.

The CFD method is based on the solution of the conservation equations for mass, momentum and energy at discrete points within a room. For a given boundary condition, numerical methods are employed to solve for the mean time temperature, pressure and velocity fields. It is also possible to determine the distribution of water vapour or pollutants, and to assess the mean age (freshness) of air at different locations within the room. Such information is the prerequisite of an appraisal of indoor air quality and discomfort.

MODEL DESCRIPTION

In recent years the application of CFD to buildings—a non-steady, mixed flow (turbulent, laminar and transitional) problem—has grown significantly (Nielsen 1989 & 1994, Jones and Whittle 1992, Denev and Stankov 2000a) and attempts have been made to combine CFD and building energy models (Negraõ 1995) or to extend CFD to include building features (Schild 1997). A building-integrated CFD model comprises six aspects: domain discretisation; a set of equations to represent the conservation of energy, mass, momentum and species; the imposition of boundary conditions; an equation solver; a method to link the CFD, building thermal and network air flow models; and the interpretation of results. The following sections describe the treatment of these aspects within the ESP-r system.

DOMAIN DISCRETISATION

A room is sub-divide into a number of finite volumes to allow the conservation equations for mass, momentum, energy and species concentration to be established and solved at discrete point throughout the continuous domain. Since room geometries are typically orthogonal, the three dimensional gridding technique shown in figure 1 has been employed. Each dimension is divided

into a number of regions, here 3 in the x-direction and 2 in the z-direction (the y-direction is not shown). These regions are then gridded using a constant or variable spacing evaluated from

$$x_i = L(i/n)^{\,c}$$

where x_i is the co-ordinate of grid line i, L the overall dimension of the region, n the number of grid lines and c a power law coefficient. Where $c > 1$, the grid starts fine and becomes course as i increases, with $c < 1$ defining the opposite scenario.

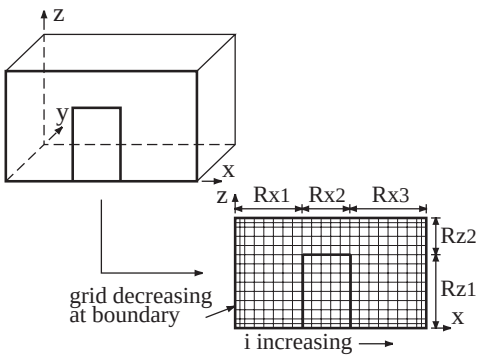

Figure 1: Room discretisation.

The scheme of table 1 has been implemented to control the gridding process. For the case of non-orthogonal geometries (figure 2), or where internal obstructions are present, the technique may be applied to an orthogonal bounding box but with the boundary of the non-participating cells treated as solid surfaces and assigned a boundary condition. To further accommodate the range of commonly encountered room shapes, the z-direction may be made non-orthogonal (Denev and Stankov 2000b).

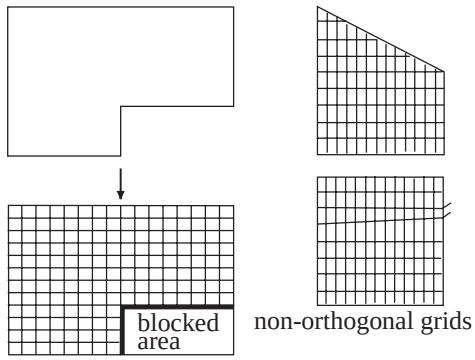

Figure 2: Treatment of non-orthogonal geometries.

CONSERVATION EQUATIONS

The movement of air within a room may be determined from the solution of the discretised mass, energy and momentum equations when subject to given boundary conditions. While these equations can be solved directly or by the technique of Large Eddy Simulation (Deardorff 1970, Davidson and Neilsen 1996), this is a computationally non-trivial task because these techniques required a fine mesh size to resolve the turbulent fluctuations. The turbulence transport technique (Rodi 1980) is therefore used whereby the instantaneous values of temperature, concentration, velocity, pressure etc may be represented as the sum of their mean and fluctuating components, and the effect of turbulent motion time-averaged. Using tensor notation, this gives rise to the following mean conservation equation for an incompressible fluid:

$$\frac{\partial}{\partial t}(\rho\phi) = \frac{\partial}{\partial x_i}\left(\Gamma_\phi \frac{\partial \phi}{\partial x_i} - \rho U_i \phi\right) + S_\phi \qquad (1)$$

where ϕ is a transport variable such as continuity ($\phi = 1$), enthalpy, concentration of contaminant or velocity; ρ the density ($kg\ m^{-3}$), Γ_ϕ a diffusion coefficient, U_i a mean velocity component (U, V, W), and S_ϕ a mean source term. The transport variables, diffusion coefficients and source terms are then as given in table 2 for each conservation equation type.

The effect of turbulent motion on the mean flow is modelled by the standard $k-\varepsilon$ model which is widely used because of its computational stability and reasonable accuracy (Launder and Spalding 1972 & 1974, Chen 1995). Its function is to determine the eddy viscosity, μ_t, of table 2 at each grid point as a function of local values of the turbulence kinetic energy (k) and its rate of dissipation (ε):

$$\mu_t = \rho C_\mu \frac{k^2}{\varepsilon}$$

where C_μ is an empirical coefficient.

The equations for k and ε are also cast in the form of eqn (1), with the diffusion and source terms as given in table 2. Because the k and ε equations contain experimentally derived parameters, the standard $k-\varepsilon$ model is fully valid only for cases of fully turbulent shear layer flow and free jets. As described later, a zero-equation (mixing length) model (Chen and Xu 1998) is used as the basis of an exploratory simulation, commissioned at each time-step, to assist with the appropriate configuring of the $k-\varepsilon$ model. This model has shown good agreement with experimental data for three test cases: natural convection with infiltration, forced convection, and mixed convection with displacement ventilation (Srebric *et al* 1999). Its attractiveness is that it does not require the solution of the k and ε equations in order to calculate the eddy viscosity. Instead, μ_t is directly related to the local mean velocity through algebraic expressions. This treatment results in a substantial reduction in the

computational burden but with the retention of reasonable accuracy in many applications (Beausoleil-Morrison 2000).

At near-wall regions where viscous effects predominate and the flow is laminar, logarithmic (log-law) wall functions are employed with the $k-\varepsilon$ model whereby the form of the velocity and temperature profile within the boundary layer is assumed in order to determine the surface shear stress and convective heat transfer (Launder and Spalding 1974). Improving this aspect of CFD is the aim of Low Reynolds Number models (Lam and Bremhorst 1981, Chien 1982, Patel *et al* 1985, Stankov and Denev 1996) with enhanced treatment of buoyancy effects (Ince and Launder 1989).

Since this convective heat transfer constitutes the pivot point between the air flow and thermal domains, any inaccuracy in its treatment will affect the entire simulation (Beausoleil-Morrison and Clarke 1998). For this reason, and depending on the outcome from the exploratory CFD run, the log-law wall functions are replaced—either by empirical heat transfer coefficients or by more applicable wall functions (e.g. for vertical walls undergoing buoyancy driven flow wall functions by Yuan *et al* (1993) are used).

Equations (1) may be discretised by standard methods to obtain a set of linear equations of the form

$$a_p\phi_p = \sum_i a_i\phi_i + b$$

where ϕ is the relevant variable of state, p designates a domain cell of interest, i designates the neighbouring cells and b relates to the source terms applied at p.

The problem therefore reduces to the solution of a set of time-averaged nodal conservation equations for U, V, W, H, C, k and ε. Because these equations are strongly coupled and highly non-linear—that is the equation coefficients and source terms are dependent on the state variables—they are solved iteratively for a given set of boundary conditions. Moreover, within an integrated simulation, the equation-sets corresponding to the building thermal, network air flow and CFD models must be solved together.

BOUNDARY CONDITIONS

Initial values of ρ, U_i and H are required at time $t = 0$ for all domain cells. For solid surfaces, the temperature (or flux) at points adjacent to the domain cells is required. For cells subjected to an in-flow from ventilation openings and doors/windows, the mass/momentum/energy/species exchange must be given in terms of the distribution of relevant variables of state—U, V, W, H, k, ε and C. At outlets, the normal practice is to impose a constant pressure, and the conditions $\partial U_n/\partial n = 0$, $\partial H/\partial n = 0$, $\partial k/\partial n = 0$, $\partial\varepsilon/\partial n = 0$, where n indicates the direction normal to the boundary. Within an integrated simulation, these data can be determined from the solution of equations corresponding to the building thermal and network flow models.

SOLUTION PROCEDURE

The SIMPLE-Consistent (SIMPLEC; Van Doormal and Raithby 1984) method is used to solve the flow equations. This method is similar to the SIMPLE (Semi-Implicit Method for Pressure-Linked Equations) method (Patankar 1980) but has less onerous simplifications applied to the momentum/continuity equations in order to obtain the pressure field correction. It is therefore more accurate.

Essentially, the pressure of each domain cell is linked to the velocities connecting with surrounding cells in a manner that conserves continuity. The method then accounts for the absence of an equation for pressure by establishing a modified form of the continuity equation to represent the pressure correction that would be required to ensure that the velocity components determined from the momentum equations move the solution towards continuity. This is done by using a guessed pressure field to solve the momentum equations for intermediate velocity components U, V and W. These velocities are then used to estimate the required pressure field correction from the modified continuity equation. The nature of this modifications, and the simplifications applied in the process, are detailed elsewhere (Versteeg and Malalasekera 1995). The energy equation, and any other scalar equations (e.g. for concentration), are then solved and the process iterates until convergence is attained. To avoid numerical divergence, under relaxation is applied to the pressure correction terms. The concentration distribution data is then post-processed to obtain the local mean age of air (freshness) using the method of Sandberg (1981).

Where the CFD domain is connected to a flow network, both solvers operate in tandem with iteration used to handle the case of strong interactions.

EQUATION-SET LINKING

The solvers for the building thermal, HVAC, network air flow and CFD equations act co-operatively. This required a conflation controller (Beausoleil-Morrison 2000) to ensure that the

CFD model is appropriately configured at each time-step.

At the start of a time-step, the zero-equation turbulence model is employed in investigative mode to determine the likely flow regimes at each surface. The eddy viscosity distribution to result is then used to initialise the k and ε fields and a second simulation performed for the time-step. This process repeats at each computational time-step.

The nature of the flow at each surface is evaluated from the local Grashof (Gr) and Reynolds (Re) Numbers as determined from the investigative simulation. The Grashof Number (the ratio of the buoyancy and viscous forces) indicates how buoyant the flow is adjacent to the surface, while the Reynolds Number (the ratio of the inertial and viscous forces) indicates how forced is the flow. The following conditions are relevant:

$Gr/\mathrm{Re}^2 \ll 1$: forced convection effects overwhelm free convection.

$Gr/\mathrm{Re}^2 \gg 1$: free convection effects dominate.

$Gr \approx \mathrm{Re}^2$: both forced and free convection effects are significant.

Based on the outcome, the following procedure is invoked.

Where buoyancy forces are insignificant, the buoyancy term in the z-momentum equation is dropped to improve solution convergence.

Where free convection predominates, the log-law wall functions are replaced by the Yuan *et al* (1993) wall functions and a Dirichlet† boundary condition imposed where the surface is vertical; otherwise a convection coefficient correlation is prescribed and a Neumann† boundary condition imposed (this means that the thermal domain will influence the flow domain but not the reverse).

Where convection is mixed, the log-law wall functions are replaced by a prescribed convection coefficient and a Robin† boundary condition imposed.

Where forced convection predominates, the ratio of the eddy viscosity to the molecular viscosity (μ_t/μ), as determined from the investigative simulation, is examined to determine how turbulent the flow is locally:

$\mu_t/\mu \leq 30$:- the flow is weakly turbulent; the log-law wall functions are replaced by a prescribed convection coefficient and a Neumann boundary condition is imposed;

$\mu_t/\mu > 30$:- the log-law wall functions are retained and a Dirichlet boundary condition is imposed.

The iterative solution of the flow equations is initiated for the current time-step. For surfaces where h_c correlations are active, these are shared with the building model so that the surface heat flux is imposed on the CFD solution. Where such correlations are not active, the CFD-derived convection coefficients are inserted into the building model's surface energy balance equations.

Where an air flow network is active, the network node representing the room is removed and new network connections are added to effect a coupling with the appropriate domain cell(s) (Negraõ 1995, Clarke *et al* 1995) as shown in figure 3. A special device has been established to ensure the accurate representation of both mass and momentum exchange between domain cells and network flow components of dissimilar size (Denev 1995). The appropriate network connection's area is increased or reduced to achieve a match with the corresponding domain cell(s) and then the associated velocity is adjusted to maintain the correct flow rate. Within the solution process, the adjusted velocity is imposed as a boundary condition to satisfy the flow rate and then it is readjusted in the momentum equation to give the correct momentum. From the viewpoint of the flow network, the air exchanges with the CFD domain are treated as sources or sinks of mass at appropriate points within the flow network solution.

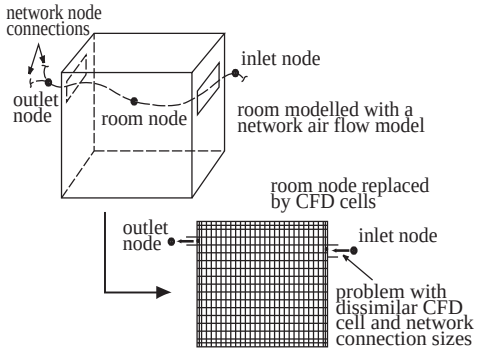

Figure 3: Coupling network flow and CFD models.

The foregoing procedure is embedded within a higher level controller that acts to synchronise the customised solvers for the building, HVAC, network flow and CFD equation-sets (figure 4). Note that the frequency of invocation of these solvers may differ. For example, in order to reduce the computational burden, the building-side solver can be invoked less frequently than the HVAC solver. Note also that that iteration may be invoked to resolve problematic coupling between domain.

It is also possible to operate on the basis of partially matched schemes. For example, the

† Dirichlet condition: fixed temperature $\theta = \theta_s$.
Neumann condition: fixed heat flux $k\,\frac{\partial\theta}{\partial n} = q$.
Robin condition: heat flux proportional to the local heat transfer $k\,\frac{\partial\theta}{\partial n} = h_c(\theta - \theta_s)$.

building model might comprise several zones, with only a subset addressed by CFD. At the same time, a flow network may be linked to one or more CFD domains, have nodes in common with some, but not all, of the other zones comprising the building model and have extra nodes to represent zones and/or plant components that are outwith the modelled building portion. Each part of such a model would then operate on the basis of best available information (e.g. a zone with no matched air flow model would utilise its user-specified infiltration/ventilation rates).

RESULTS INTERPRETATION

On the basis of the multi-variate outputs from an integrated simulation, the spatial and temporal variation of indoor air quality and thermal discomfort may be assessed according to standards prENV 1752, ISO EN 7730 and ANSI/ASHRAE 55-1992. Such an assessment is based on a set of relevant indicators:

1. the variation in vertical air temperature between floor and head height;
2. the absolute temperature of the floor;
3. radiant temperature asymmetry;
4. unsatisfactory ventilation rate;
5. unsatisfactory CO_2 level;
6. local draught assessed on the basis of the turbulence intensity distribution;
7. additional air speed required to off-set an elevated temperature;
8. comfort check based on effective temperature.
9. mean age of air.

Figure 5 gives an example output showing the distribution of air mean age for a 2D room slice. Taken together, the above outputs allow indoor regions to be differentiated in terms of air temperature, radiant asymmetry, humidity, contaminant level and air freshness, with various composite indices used to quantify standards of performance.

CONCLUSIONS

The CFD module of the ESP-r integrated modelling package has been refined as part of a collaborative research project funded by the European Commission (ERB IC15 CT98 0511) with inputs from related projects. These refinements were concerned with the treatment of complex geometries, blockages (furnishings, equipment etc), buoyancy, ventilation openings, surface heat transfer and the assessment of the spatial and temporal variation of thermal comfort and indoor air quality.

ACKNOWLEDGEMENTS

The authors are indebted to the European Commission for their invaluable support, and to our project colleagues who serviced the validation aspects of the project (Bartak *et al* 2001).

REFERENCES

Bartak M, Cermak M, Clarke J A, Denev J, Drkal F, Lain M, Macdonald I A, Majer M and Stankov P 2001 Experimental and numerical study of local mean age of air *Proc. Building Simulation 2001* (Rio de Janeiro)

Beausoleil-Morrison I 2000 The Adaptive Coupling of Heat and Air Flow Modelling within Dynamic Whole-Building Simulation *PhD Thesis* (Glasgow: University of Strathclyde)

Beausoleil-Morrison I and Clarke J 1998 The Implications of Using the Standard $k-\varepsilon$ Turbulence Model to Simulate Room Air Flows which are not Fully Turbulent *Proc. ROOMVENT '98* 99-106 (Stockholm)

Chien K-Y 1982 Predictions of Channel and Boundary-Layer Flows with a Low-Reynolds-Number Turbulence Model *AIAA Journal* **20**(1) 33-8

Clarke J A, Dempster W M and Negraõ C 1995 The Implementation of a Computational Fluid Dynamics Algorithm within the ESP-r System *Proc. Building Simulation '95* 166-75 (Madison)

Clarke J A and Hensen J L M 1991 An Approach to the Simulation of Coupled Heat and Mass Flows in Buildings *Indoor Air* **3** 283-96

Chen Q 1995 Comparison of Different $k-\varepsilon$ Models for Indoor Air Flow Computations *Numerical Heat Transfer* **B**(28) 353-69

Chen Q and Xu W 1998 A Zero-Equation Turbulence Model for Indoor Airflow Simulation *Energy and Buildings* **28**(2) 137-44

Davidson L and Neilsen P V 1996 Large Eddy Simulations of the Flow in a Three-Dimensional Ventilated Room *Proc. ROOMVENT '96* **2** 161-8 (Yokohama)

Deardorff J W 1970 A Numerical Study of Three-Dimensional Turbulent Channel Flow at Large Reynolds Numbers *J. Fluid Mech.* **42** 453-80

Denev J A 1995 Boundary conditions related to near-inlet regions and furniture in ventilated rooms *Proc. Application of Mathematics in Engineering and Business* 243-8 (Sofia: Institute of Applied Mathematics and Informatics, Technical University)

Denev J A and Stankov P 2000a Indoor climate assessment using computer simulation of air flow in a ventilated room *Journal of Theoretical and Applied Mechanics* **31**(1)

Denev J A and Stankov P 2000b Non-Orthogonal Grid Generation Techniques Applied to Room Airflow Modeling *Proc. 26th Summer School on Applications of Mathematics in Engineering and Economics (Sozopol)*

Ince N Z and B E Launder 1989 On the computation of buoyancy-driven turbulent flows in rectangular enclosures *Int. J. Heat and Fluid Flow* **10**(2) 110-7

Jones P J and Whittle G E 1992 Computational fluid dynamics for building air flow prediction - current status and capabilities *Building and Environment* **21**(3) 321-38

Lam C K G and Bremhorst K A 1981 Modified form of the $k-\varepsilon$ model for predicting wall turbulence *J. of Fluids Engng* **103** 456-60

Launder B E and Spalding D B 1972 *Mathematical Models of Turbulence* (New York: Academic)

Launder B E and Spalding D B 1974 The Numerical Computation of Turbulent Flows *Computer Methods in Applied Mechanics and Engineering* **3** 269-89

Negraõ C O R 1995 Conflation of computational fluid dynamics and building thermal simulation *PhD Thesis* (Glasgow: University of Strathclyde)

Nielsen P V 1989 Airflow Simulation Techniques Progress and Trends *Proc. 10th AIVC Conf.* 203-23

Nielsen P V 1994 Air Distribution in Rooms-Research and Design Methods *Proc. ROOMVENT '94* Krakow, Poland, V1, 15-35.

Patankar S V 1980 *Numerical heat transfer and fluid flow* (Hemisphere)

Patel V C, Rodi W and Scheuerer G 1985 Turbulence models for near-wall and low Reynolds number flows: A review *AIAA Journal* **23** 1308-19

Rodi W 1980 Turbulence Models and their Applications in Hydraulics—A State of the Art Review (Delft: Int. Association for Hydraulic Research)

Sandberg M 1981 What is ventilation efficiency? *Building and Environment* **16** 123-35

Schild P 1997 Accurate Prediction of Indoor Climate in Glazed Enclosures *PhD Thesis* (Trondheim: Norwegian University of Science and Technology)

Srebric J, Chen Q and Glicksman L R 1999 Validation of a Zero-Equation Turbulence Model for Complex Indoor Airflow Simulation *ASHRAE Trans.* **105**(2)

Stankov P and Denev J 1996 Turbulence modelling of low Reynolds number effects in 3D ventilated rooms *Proc. HERMIS'96 695-702 (Athens) ISBN 960-85176-5-6*

Versteeg H K and Malalasekera W 1995 An introduction to Computational Fluid Dynamics: The Finite Volume Method (Harlow, England: Longman)

Yuan X, Moser A and Suter P 1993 Wall Functions for Numerical Simulation of Turbulent Natural Convection Along Vertical Plates *Int. J. Heat Mass Transfer* **36**(18) 4477-85

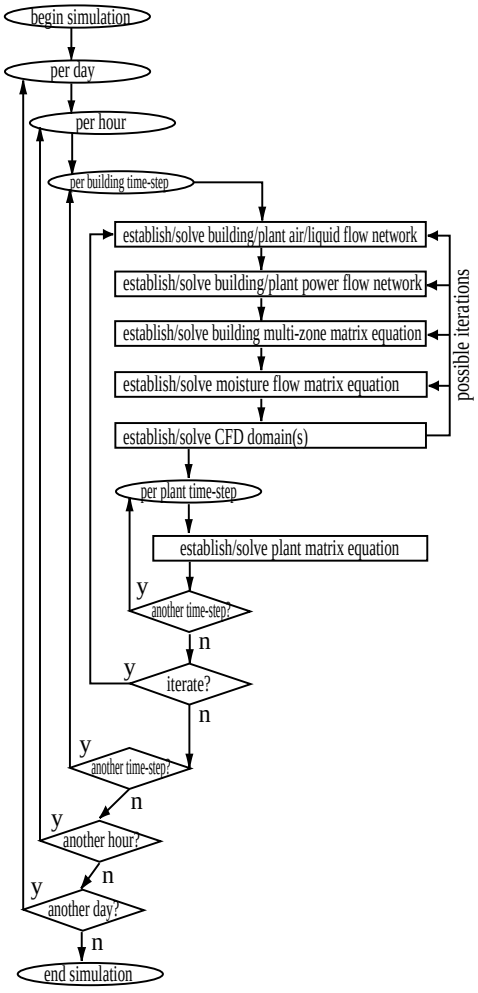

Figure 4: Iterative solution of nested domain equations.

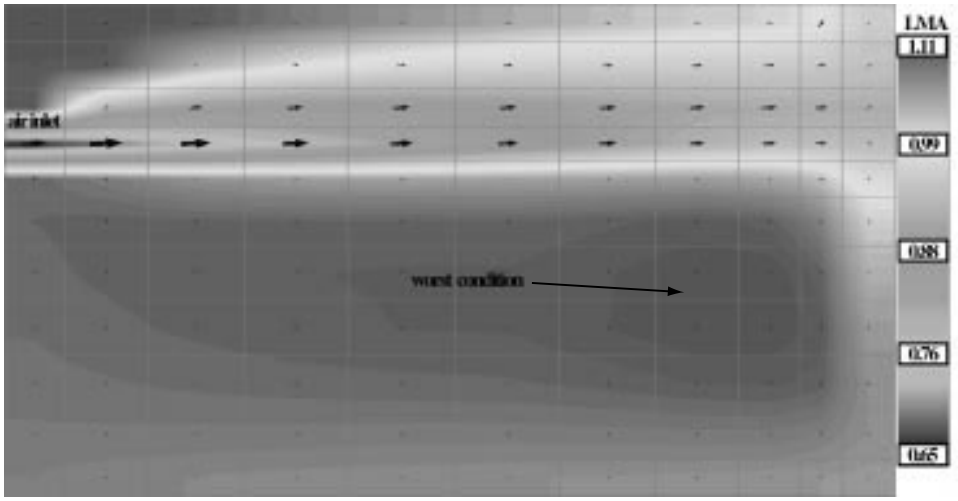

Figure 5: Distribution of the local mean age of air.

Table 1: Domain gridding parameters.

Number of grid lines in region		*Power law coefficient*	
n > 0	n cells distributed over the region	c = 1	uniform distribution
n < 0	|n| cells distributed symmetrically over the region	c > 1	increasing grid size†
		c < 1	decreasing grid size†

† From the beginning to the end (or middle if n < 0) of the region.

Table 2: Transport variables (ϕ), diffusion coefficients (Γ_ϕ) and source terms (S_ϕ).

Equation Type	ϕ	Γ_ϕ	S_ϕ
Continuity	1	-	-
Momentum	u_i	μ_{ef}	$-\frac{\partial p}{\partial x_i} - \rho g_i$
Energy	H	Γ_T	S_H
Species	C	Γ_C	S_C
Turbulent kinetic energy	k	$\frac{\mu_{ef}}{\sigma_k}$	$G - C_D \rho \varepsilon - G_b$
Dissipation rate of k	ε	$\frac{\mu_{ef}}{\sigma_\varepsilon}$	$C_1 \frac{\varepsilon}{k} G - C_2 \rho \frac{\varepsilon^2}{k} - C_3 \frac{\varepsilon}{k} G_b$

$$\Gamma_T = \frac{\mu}{Pr} + \frac{\mu_t}{\sigma_T} \quad ; \quad \Gamma_C = \frac{\mu}{Sc} + \frac{\mu_t}{\sigma_C} \quad ; \quad \mu_{ef} = \mu_t + \mu \quad ; \quad \rho = \rho(T, C)$$

$$G_b = g\left(\beta_T \frac{\mu_t}{\sigma_T} \frac{\partial T}{\partial x_i} + \beta_C \frac{\mu_t}{\sigma_C} \frac{\partial C}{\partial x_i}\right) \quad ; \quad G = \mu_t \left(\frac{\partial u_i}{\partial x_j} + \frac{\partial u_j}{\partial x_i}\right) \frac{\partial u_i}{\partial x_j}$$

$$C_D = 1.0 \quad ; \quad C_1 = 1.44 \quad ; \quad C_2 = 1.92 \quad ; \quad \sigma_k = 1.0 \quad ; \quad \sigma_\varepsilon = 1.3 \quad ; \quad \sigma_T = 0.9 \quad ; \quad \sigma_C = 0.9$$

where μ is molecular viscosity ($kg\ m^{-1}s^{-1}$), μ_t is eddy viscosity, P is pressure ($N\ m^{-2}$), g the gravitational acceleration ($m\ s^{-2}$), C_p the specific heat ($J\ kg^{-1}K^{-1}$), q''' is heat generation ($W\ m^{-3}$), Pr is the Prandtl Number, Sc is the Schmidt Number, σ_k is the turbulent energy diffusion coefficient, σ_ε is the turbulent energy dissipation diffusion coefficient, σ_T is the turbulent Prandtl Number, σ_C is the turbulent Schmidt Number, β_T is the thermal expansion coefficient (1/K).